C. R. Physique 13 (2012) 454–469

Contents lists available at SciVerse ScienceDirect

Comptes Rendus Physique

www.sciencedirect.com

Advances in nano-electromechanical systems

Decoherence suppression by cavity optomechanical cooling

Suppression de la décohérence par refroidissement optomécanique par cavité

Eyal Buks

Department of Electrical Engineering, Technion, Haifa 32000, Israel

ARTICLE INFO

Article history:
Available online 28 March 2012

Keywords:
Cavity optomechanical cooling
Decoherence suppression
Mechanical resonator

Mots-clés :
Refroidissement optomécanique par cavité
Suppression de la décohérence
Résonateur mécanique

ABSTRACT

We consider a cavity optomechanical cooling configuration consisting of a mechanical resonator (denoted as resonator b) and an electromagnetic resonator (denoted as resonator a), which are coupled in such a way that the effective resonance frequency of resonator a depends linearly on the displacement of resonator b. We study whether back-reaction effects in such a configuration can be efficiently employed for suppression of decoherence. To that end, we consider the case where the mechanical resonator is prepared in a superposition of two coherent states and evaluate the rate of decoherence. We find that no significant suppression of decoherence is achievable when resonator a is assumed to have a linear response. On the other hand, when resonator a exhibits Kerr nonlinearity and/or nonlinear damping the decoherence rate can be made much smaller than the equilibrium value provided that the parameters that characterize these nonlinearities can be tuned close to some specified optimum values.

RÉSUMÉ

Nous considérons une configuration de refroidissement optomécanique par cavité constituée par un résonateur mécanique (désigné par b) et un résonateur mécanique (désigné par a) couplés de façon que la fréquence effective de résonance du résonateur a dépend linéairement du déplacement du résonateur b. Nous étudions si la rétroaction peut être appliquée efficacement à la suppression de la décohérence dans une telle configuration. Dans ce but nous considérons le cas où le résonateur mécanique est préparé dans une superposition de deux états cohérents et nous évaluons le taux de décohérence. Nous trouvons que la décohérence ne diminue pas de façon significative si le résonateur a est supposé avoir une réponse linéaire. D'autre part, si le résonateur a présente un non-linéarité de Kerr, et/ou un amortissement non linéaire, le taux de décohérence peut devenir bien plus bas que la valeur d'équilibre, pourvu que les paramètres qui caractérisent ces non-linéarités puissent être proches de certaines valeurs optimales précises.

1. Introduction

The quest for quantum effects in nanomechanical devices has motivated an intense research effort in recent years [1–3]. Experimental demonstration of quantum superposition in a nanomechanical resonator may provide an important insight

E-mail address: eyal@ee.technion.ac.il.

1631-0705/$ – see front matter
doi:10.1016/j.crhy.2012.01.004

into the problem of quantum to classical transition [4–10]. However, in many cases the lifetime of such superposition states is too short for experimental observation since the coupling between a nanomechanical resonator and its environment typically results in rapid decoherence [11,12]. As a case study, consider a superposition of two coherent states $|\alpha_1\rangle$ and $|\alpha_2\rangle$ of a mechanical resonator having an angular resonance frequency ω_b and damping rate γ_b. The decoherence rate of such a superposition state is given in the high temperature limit $k_B T \gg \hbar\omega_b$ by [13–16]

$$\frac{1}{\tau_\varphi} = 4\gamma_b |\delta_\alpha|^2 \frac{k_B T}{\hbar\omega_b} \tag{1}$$

where $\delta_\alpha = \alpha_2 - \alpha_1$.

While Eq. (1) was derived by assuming a linear response, it is well known that nonlinear response can be exploited for reduction of thermal fluctuations. One example is the technique of noise squeezing that can be employed for reducing thermal fluctuations in one of the quadratures of a mechanical resonator [17,18]. Another example, which is the focus of this paper, is the technique of optomechanical cavity cooling. This technique [19–26], which was first proposed as a way to enhance the detection sensitivity of gravity waves [27,28], can be employed for significantly reducing the energy fluctuations of a mechanical resonator well below the equilibrium value [29–42]. Cooling is achieved by coupling the mechanical resonator (denoted as resonator b) to an electromagnetic resonator (denoted as resonator a) in such a way that the effective resonance frequency of resonator a becomes linearly dependent on the displacement of resonator b. When the parameters of the system are optimally chosen the fluctuations of resonator b around steady state can be significantly reduced well below the equilibrium value by externally driving resonator a with a monochromatic pump tone. In this region back reaction due to the retarded response of the driven resonator a to fluctuations of resonator b acts as a negative feedback, providing thus additional damping which results in effective cooling down of resonator b. The success of these experiments raises the question whether similar back-reaction effects can also be efficiently employed for suppression of decoherence below the equilibrium value.

Here we study this problem by generalizing Eq. (1) for the case where cavity cooling is applied. Nonlinearity in resonator a is taken into account to the lowest nonvanishing order. The equations of motion of the system are obtained using the Gardiner and Collett input–output theory [43,44]. By linearizing these equations we derive the susceptibility matrices of the system, which allow calculating the response of both resonators to input noise. This, in turn, allows evaluating both, the spectral density of fluctuations and the decoherence rate $1/\tau_\varphi$ of resonator b. In both cases we examine the cooling efficiency by defining an appropriate effective temperature and by calculating it for an optimum choice of the system's parameters. We find that only modest suppression of decoherence is possible using cavity cooling unless the system is driven into the region of nonlinear oscillations.

2. The model

The model consists of two resonators, labeled as a and b respectively, which are coupled to each other by a term $\hbar\Omega N_a(A_b + A_b^\dagger)$ in the Hamiltonian. Here A_a, $A_a^\dagger$ and $N_a = A_a^\dagger A_a$ (A_b, $A_b^\dagger$ and $N_b = A_b^\dagger A_b$) are respectively annihilation, creation and number operators of resonator a (b). The first resonator is coupled to 3 semi-infinite transmission lines. The first, denoted as $a1$, is a feedline, which is linearly coupled to resonator a with a coupling magnitude γ_{a1} and a coupling phase ϕ_{a1}, and which is employed to deliver the input and output signals; the second, denoted as $a2$, is linearly coupled to resonator a with a coupling magnitude γ_{a2} and a coupling phase ϕ_{a2}, and it is used to model linear dissipation, whereas the third one, denoted as $a3$, is nonlinearly coupled to resonator a with a coupling magnitude γ_{a3} and a coupling phase ϕ_{a3}, and is employed to model nonlinear dissipation. Linear dissipation of resonator b is modeled using semi-infinite transmission line, which is denoted as b and which is linearly coupled to resonator b with a coupling magnitude γ_b and coupling phase ϕ_b. Note that all coupling parameters are assumed to be ω independent. Kerr-like nonlinearity of the driven resonator a is taken into account to lowest order by including the term $(\hbar/2)K_a A_a^\dagger A_a^\dagger A_a A_a$ in the Hamiltonian of the system, which is given by

$$\begin{aligned}
\mathcal{H} = {} & \hbar\omega_a N_a + \frac{\hbar}{2} K_a A_a^\dagger A_a^\dagger A_a A_a + \hbar\omega_b N_b + \hbar\Omega N_a\left(A_b + A_b^\dagger\right) + \hbar\int \mathrm{d}\omega\, a_{a1}^\dagger(\omega) a_{a1}(\omega)\omega \\
& + \hbar\sqrt{\frac{\gamma_{a1}}{\pi}} \int \mathrm{d}\omega \left[e^{i\phi_{a1}} A_a^\dagger a_{a1}(\omega) + e^{-i\phi_{a1}} a_{a1}^\dagger(\omega) A_a\right] + \hbar\int \mathrm{d}\omega\, a_{a2}^\dagger(\omega) a_{a2}(\omega)\omega \\
& + \hbar\sqrt{\frac{\gamma_{a2}}{\pi}} \int \mathrm{d}\omega \left[e^{i\phi_{a2}} A_a^\dagger a_{a2}(\omega) + e^{-i\phi_{a2}} a_{a2}^\dagger(\omega) A_a\right] + \hbar\int \mathrm{d}\omega\, a_{a3}^\dagger(\omega) a_{a3}(\omega)\omega \\
& + \hbar\sqrt{\frac{\gamma_{a3}}{2\pi}} \int \mathrm{d}\omega \left[e^{i\phi_{a3}} A_a^\dagger A_a^\dagger a_{a3}(\omega) + e^{-i\phi_{a3}} a_{a3}^\dagger(\omega) A_a A_a\right] + \hbar\int \mathrm{d}\omega\, a_b^\dagger(\omega) a_b(\omega)\omega \\
& + \hbar\sqrt{\frac{\gamma_b}{\pi}} \int \mathrm{d}\omega \left[e^{i\phi_b} A_b^\dagger a_b(\omega) + e^{-i\phi_b} a_b^\dagger(\omega) A_b\right]
\end{aligned} \tag{2}$$

2.1. Rotating frame

The equations of motion of A_a and A_b are obtained using the Gardiner and Collett input–output theory [43,44]

$$\frac{dA_a}{dt} = -\left[i\omega_a + \gamma_a + (iK_a + \gamma_{a3})N_a\right]A_a - i\Omega A_a\left(A_b + A_b^\dagger\right) - i\sqrt{2\gamma_{a1}}e^{i\phi_{a1}}a_{a1}^{in}(t) - i\sqrt{2\gamma_{a2}}e^{i\phi_{a2}}a_{a2}^{in}(t) - 2i\sqrt{\gamma_{a3}}e^{i\phi_{a3}}A_a^\dagger a_{a3}^{in}(t) \tag{3}$$

and

$$\frac{dA_b}{dt} = -(i\omega_b + \gamma_b)A_b - i\Omega N_a - i\sqrt{2\gamma_b}e^{i\phi_b}a_b^{in}(t) \tag{4}$$

where

$$\gamma_a = \gamma_{a1} + \gamma_{a2} \tag{5}$$

and where a_{a1}^{in}, a_{a2}^{in}, a_{a3}^{in}, and a_b^{in} are input operators [43], e.g.

$$a_{a1}^{in}(t) = \frac{1}{\sqrt{2\pi}}\int d\omega\, a_{a1}(\omega, t_0)e^{i\omega(t_0-t)} \tag{6}$$

Consider the case where a coherent tone at angular frequency ω_p and a constant complex amplitude b_p is injected into the feedline. The operators of the driven resonator and its thermal baths are expressed in a frame rotating at frequency ω_p as

$$a_{a1}^{in} = B_p e^{-i\omega_p t} + c_{a1}^{in}e^{-i\omega_p t} \tag{7}$$

$$a_{a2}^{in} = c_{a2}^{in}e^{-i\omega_p t} \tag{8}$$

$$a_{a3}^{in} = c_{a3}^{in}e^{-i\omega_p t} \tag{9}$$

$$A_a = C_a e^{-i\omega_p t} \tag{10}$$

Using this notation Eqs. (3) and (4) can be rewritten as

$$\frac{dC_a}{dt} + \Theta_a = F_a \tag{11}$$

$$\frac{dA_b}{dt} + \Theta_b = F_b \tag{12}$$

where

$$\Theta_a = \Theta_a\left(C_a, C_a^\dagger, A_b, A_b^\dagger\right) = \left\{i\left[\Delta_a + \Omega\left(A_b + A_b^\dagger\right)\right] + \gamma_a + (iK_a + \gamma_{a3})N_a\right\}C_a + i\sqrt{2\gamma_{a1}}e^{i\phi_{a1}}b_p \tag{13}$$

$$\Delta_a = \omega_a - \omega_p \tag{14}$$

$$F_a = -i\sqrt{2\gamma_{a1}}e^{i\phi_{a1}}c_{a1}^{in} - i\sqrt{2\gamma_{a2}}e^{i\phi_{a2}}c_{a2}^{in} - 2i\sqrt{\gamma_{a3}}e^{i(\phi_{a3}+\omega_p t)}C_a^\dagger c_{a3}^{in} \tag{15}$$

$$\Theta_b = \Theta_b\left(C_a, C_a^\dagger, A_b, A_b^\dagger\right) = (i\omega_b + \gamma_b)A_b + i\Omega N_a \tag{16}$$

and

$$F_b = -i\sqrt{2\gamma_b}e^{i\phi_b}a_b^{in}(t) \tag{17}$$

3. Linearization

Expressing the solution as

$$C_a = B_a + c_a \tag{18a}$$

$$A_b = B_b + c_b \tag{18b}$$

where both B_a and B_b are complex numbers, and considering both c_a and c_b as small one has to lowest order

$$\Theta_a\left(C_a, C_a^\dagger, C_b, C_b^\dagger\right) = \Theta_a\left(B_a, B_a^*, B_b, B_b^*\right) + W_1 c_a + W_2 c_a^\dagger + W_3 c_b + W_4 c_b^\dagger \tag{19}$$

$$\Theta_b\left(C_a, C_a^\dagger, C_b, C_b^\dagger\right) = \Theta_b\left(B_a, B_a^*, B_b, B_b^*\right) + W_5 c_a + W_6 c_a^\dagger + W_7 c_b + W_8 c_b^\dagger \tag{20}$$

where

$$W_1 = i\Delta_a^{\text{eff}} + \gamma_a + 2(iK_a + \gamma_{a3})|B_a|^2 \tag{21a}$$

$$W_2 = (iK_a + \gamma_{a3})B_a^2 \tag{21b}$$

$$W_3 = W_4 = i\Omega B_a \tag{21c}$$

$$W_5 = i\Omega B_a^* \tag{21d}$$

$$W_6 = i\Omega B_a \tag{21e}$$

$$W_7 = i\omega_b + \gamma_b \tag{21f}$$

$$W_8 = 0 \tag{21g}$$

and where

$$\Delta_a^{\text{eff}} = \Delta_a + \Omega\left(B_b + B_b^*\right) \tag{22}$$

3.1. Mean field solution

Mean field solutions are found by solving

$$\Theta_a\left(B_a, B_a^*, B_b, B_b^*\right) = 0 \tag{23a}$$

$$\Theta_b\left(B_a, B_a^*, B_b, B_b^*\right) = 0 \tag{23b}$$

that is

$$\left[i\Delta_a^{\text{eff}} + \gamma_a + (iK_a + \gamma_{a3})|B_a|^2\right]B_a + i\sqrt{2\gamma_{a1}}e^{i\phi_{a1}}b_{\text{p}} = 0 \tag{24}$$

and

$$(i\omega_b + \gamma_b)B_b + i\Omega|B_a|^2 = 0 \tag{25}$$

Extracting B_b from Eq. (25) and substituting it in Eq. (24) yields

$$\left\{i\Delta_a + \gamma_a + \left(iK_a^{\text{eff}} + \gamma_{a3}\right)|B_a|^2\right\}B_a + i\sqrt{2\gamma_{a1}}e^{i\phi_{a1}}b_{\text{p}} = 0 \tag{26}$$

where K_a^{eff}, which is given by

$$K_a^{\text{eff}} = K_a - \frac{2\Omega^2\omega_b}{\omega_b^2 + \gamma_b^2} \tag{27}$$

is the effective Kerr constant. Taking the module squared of Eq. (26) leads to

$$\left[\left(\Delta_a + K_a^{\text{eff}}E_a\right)^2 + (\gamma_a + \gamma_{a3}E_a)^2\right]E_a = 2\gamma_{a1}|b_{\text{p}}|^2 \tag{28}$$

where

$$E_a = |B_a|^2 \tag{29}$$

Finding E_a by solving Eq. (28) allows calculating B_a according to Eq. (26) and B_b according to Eq. (25).

3.2. Onset of the bistability point

In general, for any fixed value of the driving amplitude b_{p}, Eq. (26) can be expressed as a relation between E_a and Δ_a. When b_{p} is sufficiently large the response of the system becomes bistable, that is E_a becomes a multi-valued function of Δ_a in some range near the resonance frequency. The onset of the bistability point is defined as the point for which

$$\frac{\partial\Delta_a}{\partial E_a} = 0 \tag{30}$$

$$\frac{\partial^2\Delta_a}{\partial(E_a)^2} = 0 \tag{31}$$

Such a point occurs only if the nonlinear damping is sufficiently small [44], namely, only when the following condition holds

$$\left|K_a^{\text{eff}}\right| > \sqrt{3}\gamma_{a3} \tag{32}$$

At the onset of the bistability point the driving frequency and amplitude are given by

$$(\Delta_a)_c = -\gamma_a \frac{K_a^{\rm eff}}{|K_a^{\rm eff}|}\left[\frac{4\gamma_{a3}|K_a^{\rm eff}| + \sqrt{3}((K_a^{\rm eff})^2 + \gamma_{a3}^2)}{(K_a^{\rm eff})^2 - 3\gamma_{a3}^2}\right] \tag{33}$$

$$(b_{\rm p})_c^2 = \frac{4}{3\sqrt{3}} \frac{\gamma_a^3((K_a^{\rm eff})^2 + \gamma_{a3}^2)}{\gamma_{a1}(|K_a^{\rm eff}| - \sqrt{3}\gamma_{a3})^3} \tag{34}$$

and the resonator mode amplitude is

$$(E_a)_c = \frac{2\gamma_a}{\sqrt{3}(|K_a^{\rm eff}| - \sqrt{3}\gamma_{a3})} \tag{35}$$

3.3. Fluctuation

Fluctuations around the mean field solution are governed by

$$\frac{\rm d}{{\rm d}t}\begin{pmatrix} c_a \\ c_a^\dagger \\ c_b \\ c_b^\dagger \end{pmatrix} + W\begin{pmatrix} c_a \\ c_a^\dagger \\ c_b \\ c_b^\dagger \end{pmatrix} = \begin{pmatrix} F_a \\ F_a^\dagger \\ F_b \\ F_b^\dagger \end{pmatrix} \tag{36}$$

where the matrix W is given by

$$W = \begin{pmatrix} W_1 & W_2 & W_3 & W_4 \\ W_2^* & W_1^* & W_4^* & W_3^* \\ W_5 & W_6 & W_7 & W_8 \\ W_6^* & W_5^* & W_8^* & W_7^* \end{pmatrix} \tag{37}$$

The mean field solution is assumed to be locally stable, that is, it is assumed that all eigenvalues of W have a positive real part.

By assuming that the bath mode is in thermal equilibrium one finds with the help of Eqs. (6)–(10), (15) and (17) that

$$\left\langle F_a(\omega)F_a^\dagger(\omega')\right\rangle = 2\Gamma_a\delta(\omega-\omega')n_{\omega_a} \tag{38}$$

$$\left\langle F_a^\dagger(\omega)F_a(\omega')\right\rangle = 2\Gamma_a\delta(\omega-\omega')(n_{\omega_a}+1) \tag{39}$$

$$\left\langle F_b(\omega)F_b^\dagger(\omega')\right\rangle = 2\gamma_b\delta(\omega-\omega')n_{\omega_b} \tag{40}$$

and

$$\left\langle F_b^\dagger(\omega)F_b(\omega')\right\rangle = 2\gamma_b\delta(\omega-\omega')(n_{\omega_b}+1) \tag{41}$$

where $n_\omega = (e^{\beta\hbar\omega}-1)^{-1}$, $\beta = 1/k_{\rm B}T$, $k_{\rm B}$ is Boltzmann's constant and T is the absolute temperature and where

$$\Gamma_a = \gamma_a + 2\gamma_{a3}E_a \tag{42}$$

It is important to note that the linearization approach is valid only when the fluctuations around the mean field solution are small. Unavoidably, however, very close to the region where the system becomes unstable the fluctuations become appreciable, and consequently the linearization approximation breaks down.

3.4. Transforming into Fourier space

In general, the Fourier transform of a time dependent operator $O(t)$ is denoted as $O(\omega)$

$$O(t) = \frac{1}{\sqrt{2\pi}}\int_{-\infty}^{\infty} {\rm d}\omega\, O(\omega)e^{-i\omega t} \tag{43}$$

Applying the Fourier transform to Eq. (36) yields

$$W_{aa}\begin{pmatrix} c_a(\omega) \\ c_a^\dagger(-\omega) \end{pmatrix} + W_{ab}\begin{pmatrix} c_b(\omega) \\ c_b^\dagger(-\omega) \end{pmatrix} = \begin{pmatrix} F_a(\omega) \\ F_a^\dagger(-\omega) \end{pmatrix} \tag{44}$$

$$W_{ba}\begin{pmatrix} c_a(\omega) \\ c_a^\dagger(-\omega) \end{pmatrix} + W_{bb}\begin{pmatrix} c_b(\omega) \\ c_b^\dagger(-\omega) \end{pmatrix} = \begin{pmatrix} F_b(\omega) \\ F_b^\dagger(-\omega) \end{pmatrix} \tag{45}$$

where

$$W_{aa} = \begin{pmatrix} W_1 - i\omega & W_2 \\ W_2^* & W_1^* - i\omega \end{pmatrix} \tag{46}$$

$$W_{ab} = \begin{pmatrix} W_3 & W_4 \\ W_4^* & W_3^* \end{pmatrix} \tag{47}$$

$$W_{ba} = \begin{pmatrix} W_5 & W_6 \\ W_6^* & W_5^* \end{pmatrix} \tag{48}$$

$$W_{bb} = \begin{pmatrix} W_7 - i\omega & W_8 \\ W_8^* & W_7^* - i\omega \end{pmatrix} \tag{49}$$

By inverting these equations one finds that

$$\begin{pmatrix} c_a(\omega) \\ c_a^\dagger(-\omega) \end{pmatrix} = \chi_{aa}\begin{pmatrix} F_a(\omega) \\ F_a^\dagger(-\omega) \end{pmatrix} + \chi_{ab}\begin{pmatrix} F_b(\omega) \\ F_b^\dagger(-\omega) \end{pmatrix} \tag{50}$$

$$\begin{pmatrix} c_b(\omega) \\ c_b^\dagger(-\omega) \end{pmatrix} = \chi_{ba}\begin{pmatrix} F_a(\omega) \\ F_a^\dagger(-\omega) \end{pmatrix} + \chi_{bb}\begin{pmatrix} F_b(\omega) \\ F_b^\dagger(-\omega) \end{pmatrix} \tag{51}$$

where

$$\chi_{aa} = \left(W_{aa} - W_{ab}W_{bb}^{-1}W_{ba}\right)^{-1} \tag{52a}$$

$$\chi_{ab} = \left(W_{ba} - W_{bb}W_{ab}^{-1}W_{aa}\right)^{-1} \tag{52b}$$

$$\chi_{ba} = \left(W_{ab} - W_{aa}W_{ba}^{-1}W_{bb}\right)^{-1} \tag{52c}$$

$$\chi_{bb} = \left(W_{bb} - W_{ba}W_{aa}^{-1}W_{ab}\right)^{-1} \tag{52d}$$

3.5. Omega-symmetric matrix

Let $W(\omega)$ be a 2×2 matrix, which depends on the real parameter ω. The matrix $W(\omega)$ is said to be omega-symmetric if it can be written as

$$W(\omega) = \begin{pmatrix} a(\omega) & b(\omega) \\ b^*(-\omega) & a^*(-\omega) \end{pmatrix} \tag{53}$$

where $a(\omega)$ and $b(\omega)$ are arbitrary smooth functions of ω. It is straightforward to show that if W is omega-symmetric then W^{-1}, W^t (transpose of W) and $W^\dagger$ are all omega-symmetric as well. Moreover, if W_1 and W_2 are both omega-symmetric then W_1W_2 is also omega-symmetric. Thus, it is easy to show that the susceptibility matrices χ_{aa}, χ_{ab}, χ_{ba} and χ_{bb} are all omega-symmetric.

3.6. The case where Ω is small and $K_a = \gamma_{a3} = 0$

To lowest order in Ω one has

$$\chi_{aa} = \left(1 - W_{aa}^{-1}W_{ab}W_{bb}^{-1}W_{ba}\right)^{-1}W_{aa}^{-1} \simeq \left(1 + W_{aa}^{-1}W_{ab}W_{bb}^{-1}W_{ba}\right)W_{aa}^{-1} \tag{54}$$

$$\chi_{ab} \simeq -W_{aa}^{-1}W_{ab}W_{bb}^{-1} \tag{55}$$

$$\chi_{ba} \simeq -W_{bb}^{-1}W_{ba}W_{aa}^{-1} \tag{56}$$

and

$$\chi_{bb} = \left(1 - W_{bb}^{-1}W_{ba}W_{aa}^{-1}W_{ab}\right)^{-1}W_{bb}^{-1} \simeq \left(1 + W_{bb}^{-1}W_{ba}W_{aa}^{-1}W_{ab}\right)W_{bb}^{-1} \tag{57}$$

For the case $K_a = \gamma_{a3} = 0$ one finds that

$$\chi_{aa}=\begin{pmatrix}\frac{1}{\lambda_{a1}-i\omega} & 0\\ 0 & \frac{1}{\lambda_{a2}-i\omega}\end{pmatrix}+\frac{\Omega^2\begin{pmatrix}\frac{E_a(\lambda_{b1}-\lambda_{b2})}{(\lambda_{a1}-i\omega)^2} & \frac{B_a^2(\lambda_{b1}-\lambda_{b2})}{(\lambda_{a1}-i\omega)(\lambda_{a2}-i\omega)}\\ -\frac{(B_a^*)^2(\lambda_{b1}-\lambda_{b2})}{(\lambda_{a1}-i\omega)(\lambda_{a2}-i\omega)} & -\frac{E_a(\lambda_{b1}-\lambda_{b2})}{(\lambda_{a2}-i\omega)^2}\end{pmatrix}}{(\lambda_{b1}-i\omega)(\lambda_{b2}-i\omega)} \tag{58}$$

$$\chi_{ab}=-\Omega\begin{pmatrix}\frac{iB_a}{(\lambda_{a1}-i\omega)(\lambda_{b1}-i\omega)} & \frac{iB_a}{(\lambda_{a1}-i\omega)(\lambda_{b2}-i\omega)}\\ -\frac{iB_a^*}{(\lambda_{a2}-i\omega)(\lambda_{b1}-i\omega)} & -\frac{iB_a^*}{(\lambda_{a2}-i\omega)(\lambda_{b2}-i\omega)}\end{pmatrix} \tag{59}$$

$$\chi_{ba}=-\Omega\begin{pmatrix}\frac{iB_a^*}{(\lambda_{a1}-i\omega)(\lambda_{b1}-i\omega)} & \frac{iB_a}{(\lambda_{a2}-i\omega)(\lambda_{b1}-i\omega)}\\ -\frac{iB_a^*}{(\lambda_{a1}-i\omega)(\lambda_{b2}-i\omega)} & -\frac{iB_a}{(\lambda_{a2}-i\omega)(\lambda_{b2}-i\omega)}\end{pmatrix} \tag{60}$$

and

$$\chi_{bb}=\begin{pmatrix}\frac{1}{\lambda_{b1}-i\omega} & 0\\ 0 & \frac{1}{\lambda_{b2}-i\omega}\end{pmatrix}+\frac{\Omega^2E_a\begin{pmatrix}\frac{(\lambda_{a1}-\lambda_{a2})}{(\lambda_{b1}-i\omega)^2} & \frac{(\lambda_{a1}-\lambda_{a2})}{(\lambda_{b1}-i\omega)(\lambda_{b2}-i\omega)}\\ -\frac{(\lambda_{a1}-\lambda_{a2})}{(\lambda_{b1}-i\omega)(\lambda_{b2}-i\omega)} & -\frac{(\lambda_{a1}-\lambda_{a2})}{(\lambda_{b2}-i\omega)^2}\end{pmatrix}}{(\lambda_{a1}-i\omega)(\lambda_{a2}-i\omega)} \tag{61}$$

where we have introduced the eigenvalues

$$\lambda_{a1}+\lambda_{a2}=W_1+W_1^* \tag{62a}$$

$$\lambda_{a1}\lambda_{a2}=|W_1|^2-|W_2|^2 \tag{62b}$$

and

$$\lambda_{b1}+\lambda_{b2}=W_7+W_7^* \tag{63a}$$

$$\lambda_{b1}\lambda_{b2}=|W_7|^2-|W_8|^2 \tag{63b}$$

To determine the stability of the mean field solutions the eigenvalues of W are calculated below for the present case to lowest nonvanishing order in Ω. The matrix W can be expressed as

$$W=\begin{pmatrix}\lambda_{a1} & 0 & 0 & 0\\ 0 & \lambda_{a2} & 0 & 0\\ 0 & 0 & \lambda_{b1} & 0\\ 0 & 0 & 0 & \lambda_{b2}\end{pmatrix}+\Omega V \tag{64}$$

where

$$V=\begin{pmatrix}0 & 0 & iB_a & iB_a\\ 0 & 0 & -iB_a^* & -iB_a^*\\ iB_a^* & iB_a & 0 & 0\\ -iB_a^* & -iB_a & 0 & 0\end{pmatrix}$$

The two eigenvalues of interest for what follows are $\tilde{\lambda}_{b1}$ and $\tilde{\lambda}_{b2}$, which approach the values λ_{b1} and λ_{b2} respectively in the limit $\Omega\to 0$. These eigenvalues are calculated up to second order in Ω using perturbation theory (note that W is not necessarily Hermitian)

$$\tilde{\lambda}_{b1}=\lambda_{b1}+\Omega^2E_a\left(-\frac{1}{\lambda_{b1}-\lambda_{a1}}+\frac{1}{\lambda_{b1}-\lambda_{a2}}\right) \tag{65a}$$

$$\tilde{\lambda}_{b2}=\lambda_{b2}+\Omega^2E_a\left(\frac{1}{\lambda_{b2}-\lambda_{a1}}-\frac{1}{\lambda_{b2}-\lambda_{a2}}\right) \tag{65b}$$

Thus by using the relations

$$\lambda_{a1}=\lambda_{a2}^*=i\Delta_a^{\mathrm{eff}}+\gamma_a \tag{66a}$$

$$\lambda_{b1}=\lambda_{b1}^*=i\omega_b+\gamma_b \tag{66b}$$

the notation

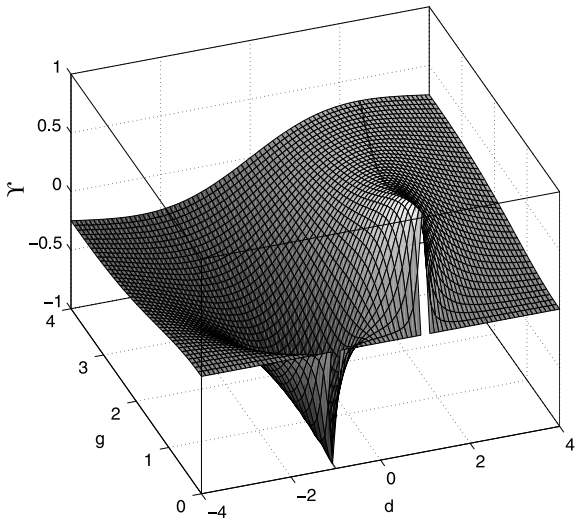

Fig. 1. The function $\Upsilon(d,g)$.

$$d=\frac{\Delta_a^{\mathrm{eff}}}{\omega_b} \tag{67a}$$

$$g=\frac{\gamma_a}{\omega_b} \tag{67b}$$

and by assuming also that $\gamma_b \ll \omega_b$ one finds that

$$\tilde{\lambda}_{b1}=i\omega_b\left(1+\frac{2\Omega^2E_a}{\omega_b^2}\frac{2d(1-d^2-g^2)}{[(d+1)^2+g^2][(d-1)^2+g^2]}\right)+\gamma_b\left(1+\frac{2\Omega^2E_a}{\gamma_a\gamma_b}\frac{4dg^2}{[(1+d)^2+g^2][(1-d)^2+g^2]}\right) \tag{68}$$

and $\tilde{\lambda}_{b2}=\tilde{\lambda}_{b1}^*$.

For the present case ($K_a=\gamma_{a3}=0$) one finds using Eqs. (27) and (35) that $(E_a)_c$ (the value of E_a at the onset of bistability) is given by

$$(E_a)_c=\frac{\gamma_a\omega_b}{\sqrt{3}\Omega^2} \tag{69}$$

In terms of $(E_a)_c$ the real part of $\tilde{\lambda}_{b1}$ can be expressed as

$$\frac{\mathrm{Re}(\tilde{\lambda}_{b1})}{\gamma_b}=1+\frac{2E_a}{\sqrt{3}(E_a)_c}\frac{\omega_b}{\gamma_b}\Upsilon(d,g) \tag{70}$$

where the function $\Upsilon(d,g)$, which is plotted in Fig. 1, is given by

$$\Upsilon(d,g)=\frac{4dg^2}{[(1+d)^2+g^2][(1-d)^2+g^2]}=\frac{4g^2d}{4g^2+(g^2-1+d^2)^2} \tag{71}$$

While the parameter d represents the detuning between the driving frequency and the resonance frequency, the parameter g, which is the ratio between the period time of resonator b and the ring-down time of resonator a, represents the level of retardation in the response of resonator a. The function $\Upsilon(d,g)$ describes the way the shift in the eigenvalues depends on these parameters. For any given value of g the function Υ obtains a maximum at $d=d_0$ and a minimum at $d=-d_0$, where

$$d_0=\frac{1}{3}\sqrt{3-3g^2+6\sqrt{g^4+g^2+1}} \tag{72}$$

The mean field solution is stable provided that $\mathrm{Re}(\tilde{\lambda}_{b1})>0$. Hopf bifurcation occurs when $\mathrm{Re}(\tilde{\lambda}_{b1})$ vanishes.

4. Integrated spectral density

In general consider an operator $c(\omega)$ that can be expressed in terms of a noise operator $F(\omega)$ and a susceptibility matrix $\chi(\omega)$ as [similarly to Eqs. (50) and (51)]

$$\begin{pmatrix} c(\omega) \\ c^\dagger(-\omega) \end{pmatrix} = \chi(\omega) \begin{pmatrix} F(\omega) \\ F^\dagger(-\omega) \end{pmatrix} \tag{73}$$

where $F(\omega)$ satisfy [similarly to Eqs. (38)–(40) and (41)]

$$\langle F(\omega) \rangle = \langle F^\dagger(\omega) \rangle = 0 \tag{74}$$

$$\langle F(\omega) F(\omega') \rangle = \langle F^\dagger(\omega) F^\dagger(\omega') \rangle = 0 \tag{75}$$

$$\langle F(\omega) F^\dagger(\omega') \rangle = 2\Gamma \delta(\omega - \omega') n_{\omega_0} \tag{76}$$

and

$$\langle F^\dagger(\omega) F(\omega') \rangle = 2\Gamma \delta(\omega - \omega')(n_{\omega_0} + 1) \tag{77}$$

The homodyne detection observable $X(\omega)$ is defined by

$$X(\omega) = e^{i\phi_{\mathrm{LO}}} c(\omega) + e^{-i\phi_{\mathrm{LO}}} c^\dagger(-\omega) \tag{78}$$

The frequency auto-correlation function of X is related to the spectral density $P_X(\omega)$ by

$$\langle X^\dagger(\omega') X(\omega) \rangle = P_X(\omega) \delta(\omega - \omega') \tag{79}$$

Assuming that $\chi(\omega)$ is omega-symmetric, it can be expressed as

$$\chi(\omega) = \begin{pmatrix} a(\omega) & b(\omega) \\ b^*(-\omega) & a^*(-\omega) \end{pmatrix} \tag{80}$$

where $a(\omega)$ and $b(\omega)$ are arbitrary functions of ω. By calculating the term $\langle X^\dagger(\omega') X(\omega) \rangle$ one finds that

$$\frac{P_X(\omega)}{2\Gamma} = M_+(\omega) \coth \frac{\beta\hbar\omega_0}{2} + M_-(\omega) \tag{81}$$

where

$$M_+(\omega) = \frac{|a(-\omega)|^2 + |b(\omega)|^2 + |a(\omega)|^2 + |b(-\omega)|^2}{2} + \mathrm{Re}\left[e^{2i\phi_{\mathrm{LO}}} \left(a(-\omega) b(\omega) + a(\omega) b(-\omega) \right) \right] \tag{82}$$

and

$$M_-(\omega) = \frac{-|a(-\omega)|^2 - |b(\omega)|^2 + |a(\omega)|^2 + |b(-\omega)|^2}{2} + \mathrm{Re}\left[e^{2i\phi_{\mathrm{LO}}} \left(-a(-\omega) b(\omega) + a(\omega) b(-\omega) \right) \right] \tag{83}$$

The integrated spectral density (ISD) is thus given by

$$\int_{-\infty}^{\infty} \mathrm{d}\omega \, P_X(\omega) = 2\Gamma V \coth \frac{\beta\hbar\omega_0}{2} \tag{84}$$

where

$$V = \int_{-\infty}^{\infty} \mathrm{d}\omega \, M_+(\omega) = \int_{-\infty}^{\infty} \mathrm{d}\omega \left[\left| a(\omega) \right|^2 + \left| b(-\omega) \right|^2 + 2\,\mathrm{Re}\left(e^{2i\phi_{\mathrm{LO}}} a(\omega) b(-\omega) \right) \right] \tag{85}$$

5. ISD of X_b

We calculate below the ISD of the homodyne observable $X_b(\omega)$, which is given by

$$X_b(\omega) = e^{i\phi_{\mathrm{LO}}} c_b(\omega) + e^{-i\phi_{\mathrm{LO}}} c_b^\dagger(-\omega) \tag{86}$$

for the case where Ω is small and $K_a = \gamma_{a3} = 0$. As can be seen from Eq. (51), it has two contributions due to the two uncorrelated noise terms $F_b(\omega)$ and $F_a(\omega)$. The calculation of both contributions according to Eq. (84) is involved with evaluation of some integrals, which can be performed using the residue theorem. To further simplify the final result, which is given by

$$\frac{1}{2\pi} \int_{-\infty}^{\infty} \mathrm{d}\omega \, P_{X_b}(\omega) = \left(1 - \frac{\Omega^2 E_a}{\gamma_a \gamma_b} \Upsilon(d, g) \right) \coth \frac{\beta\hbar\omega_b}{2} + \frac{\Omega^2 E_a}{\gamma_a \gamma_b} \frac{2g^2}{(1-d)^2 + g^2} \coth \frac{\beta\hbar\omega_a}{2} \tag{87}$$

the case where resonator b has high quality factor is assumed. For this case, which is experimentally common, the following is assumed to hold $\gamma_b \ll \omega_b$ and $\gamma_b \ll \gamma_a$. As can be seen from Eq. (87), for finite driven amplitude E_a the ISD of X_b can deviate from the equilibrium value of $\coth(\beta\hbar\omega_b/2)$.

6. Decoherence

Consider the case where resonator b is initially prepared at time $t=0$ in a superposition state of two coherent states $|\alpha_1\rangle_b$ and $|\alpha_2\rangle_b$. We employ below the approach that has been introduced in Ref. [45] to evaluate the decoherence time τ_φ of such a superposition state. The initial state of the system is taken to be given by

$$\big|\psi(t=0)\big\rangle = \big(|\alpha_1\rangle_b + |\alpha_2\rangle_b\big)\otimes|\chi_i\rangle_{\mathrm{D}} \tag{88}$$

where $|\chi_i\rangle_{\mathrm{D}}$ represents an initial state of all other degrees of freedom of the system. The time evolution of the system is determined by the Hamiltonian $\mathcal{H}$ (2), which is formally a function of A_b and $A_b^\dagger$, that is $\mathcal{H}=\mathcal{H}(A_b, A_b^\dagger)$.

For simplicity, the case where $\omega_b\tau_\varphi \ll 1$ is assumed. As can be seen from Eq. (1), in thermal equilibrium this case occurs when $|\delta_\alpha|^2 k_{\mathrm{B}} T\gamma_b/\hbar\omega_b^2 \gg 1$, where $\delta_\alpha=\alpha_2-\alpha_1$. For this case the time evolution of resonator b can be neglected on the time scale of τ_φ, and consequently for a time $t \lesssim \tau_\varphi$ the state $|\psi(t=0)\rangle$ in the Schrödinger representation will approximately evolve into

$$\big|\psi(t)\big\rangle = |\alpha_1\rangle_b\otimes u_1(t)|\chi_i\rangle_{\mathrm{D}} + |\alpha_2\rangle_b u_2(t)\otimes|\chi_i\rangle_{\mathrm{D}} \tag{89}$$

where the time evolution operator $u_1(t)$ [$u_2(t)$] is generated by the Hamiltonian $\mathcal{H}(\alpha_1,\alpha_1^*)$ [$\mathcal{H}(\alpha_2,\alpha_2^*)$].

The distinguishability between the two coherent states is characterized by the parameter

$$\nu \equiv \big|{}_{\mathrm{D}}\langle\chi_i|u_1^\dagger(t)u_2(t)|\chi_i\rangle_{\mathrm{D}}\big|^2 \tag{90}$$

Our goal is to find the characteristic time scale τ_φ over which ν decays from its initial value $\nu=1$ at time $t=0$. Regarding the parameter δ_α as small, one can evaluate ν using perturbation theory [46,47]. To lowest nonvanishing order in δ_α one finds that

$$\nu = 1-\frac{1}{\hbar^2}\int_0^t \mathrm{d}t'\int_0^t \mathrm{d}t''\big\langle\tilde{\mathcal{V}}(t')\tilde{\mathcal{V}}(t'')\big\rangle \tag{91}$$

where $\tilde{\mathcal{V}}=\mathcal{V}(t)-\langle\mathcal{V}(t)\rangle$ and where $\mathcal{V}=\mathcal{H}(\alpha_2,\alpha_2^*)-\mathcal{H}(\alpha_1,\alpha_1^*)$.

In a steady state the correlation function $\langle\tilde{\mathcal{V}}(t')\tilde{\mathcal{V}}(t'')\rangle$ is expected to be a function of $|t'-t''|$; this function is labeled as $f_{\mathcal{V}}(|t'-t''|)=\langle\tilde{\mathcal{V}}(t')\tilde{\mathcal{V}}(t'')\rangle$. In the limit where t is much larger than the correlation time, which characterizes the width of the peak in the function $f_{\mathcal{V}}(\tau)$ around the value $\tau=0$, one finds that

$$\nu \simeq 1-\frac{t}{\hbar^2}\int_{-\infty}^{\infty}\mathrm{d}\tau\, f_{\mathcal{V}}(\tau) \tag{92}$$

Thus, the rate at which the parameter ν decays (i.e. the decoherence rate $1/\tau_\varphi$) is given by

$$\frac{1}{\tau_\varphi} = \frac{1}{\hbar^2}\int_{-\infty}^{\infty}\mathrm{d}\tau\,\big\langle\tilde{\mathcal{V}}(\tau)\tilde{\mathcal{V}}(0)\big\rangle \tag{93}$$

Alternatively, in terms of the Fourier transformed function $\tilde{\mathcal{V}}(\omega)$, which is related to $\tilde{\mathcal{V}}(t)$ by

$$\tilde{\mathcal{V}}(t) = \frac{1}{\sqrt{2\pi}}\int_{-\infty}^{\infty}\mathrm{d}\omega\,\tilde{\mathcal{V}}(\omega)e^{-i\omega t} \tag{94}$$

the decoherence rate can be expressed as

$$\frac{1}{\tau_\varphi} = \frac{1}{\hbar^2}\int_{-\infty}^{\infty}\mathrm{d}\omega\big\langle\tilde{\mathcal{V}}(0)\tilde{\mathcal{V}}(\omega)\big\rangle \tag{95}$$

Using Eqs. (17) and (50) together with the notation

$$\delta_\alpha=\alpha_2-\alpha_1=|\delta_\alpha|e^{i\theta} \tag{96}$$

one finds to lowest order that

$$\frac{\tilde{\mathcal{V}}(\omega)}{\hbar|\delta_\alpha|} = U_a F_a(\omega)+U_a^* F_a^\dagger(-\omega)+U_b F_b(\omega)+U_b^* F_b^\dagger(-\omega) \tag{97}$$

where

$$U_a = 2\Omega\cos\theta\left(B_a^*(\chi_{aa})_{11} + B_a(\chi_{aa})_{21}\right) \tag{98a}$$

$$U_b = 2\Omega\cos\theta\left(B_a^*(\chi_{ab})_{11} + B_a(\chi_{ab})_{21}\right) + ie^{-i\theta} \tag{98b}$$

Furthermore, with the help of Eqs. (38)–(40) and (41) the decoherence rate becomes

$$\frac{1}{\tau_\varphi} = 2|\delta_\alpha|^2\left(\Gamma_a|U_a|^2\coth\frac{\beta\hbar\omega_a}{2} + \gamma_b|U_b|^2\coth\frac{\beta\hbar\omega_b}{2}\right) \tag{99}$$

Note that for $\Omega = 0$ the decoherence rate reproduces the value given by Eq. (1).

For the case where Ω is small and $K_a = \gamma_{a3} = 0$ one finds using Eqs. (58) and (59) that

$$|U_a|^2 = \frac{4\Omega^2 E_a\cos^2\theta}{\omega_b^2(d^2+g^2)} \tag{100}$$

and

$$|U_b|^2 = 1 + \frac{4\Omega^2 E_a[\cos a + \cos(2\theta+a)]}{\omega_b^2\sqrt{1+(\frac{\gamma_b}{\omega_b})^2}}\frac{d}{d^2+g^2} \tag{101}$$

where

$$a = \tan^{-1}\frac{\gamma_b}{\omega_b} \tag{102}$$

In what follows we restrict the discussion to the case where $\theta = 0$, for which the two coherent states $|\alpha_1\rangle$ and $|\alpha_2\rangle$ have the same momentum. For this case, which is the assumed case in some of the published proposals for observation of quantum superposition in mechanical systems [8,9,48], up to first order in γ_b/ω_b one has

$$|U_b|^2 = 1 + \frac{4\Omega^2 E_a}{\omega_b^2}\frac{d}{d^2+g^2} \tag{103}$$

Using these results together with Eq. (99) one finds that

$$\frac{1}{\tau_\varphi} = 2\gamma_b|\delta_\alpha|^2\left[\left(1+\frac{4\Omega^2 E_a}{\omega_b^2}\frac{d}{d^2+g^2}\right)\coth\frac{\beta\hbar\omega_b}{2} + \frac{\gamma_a}{\gamma_b}\frac{4\Omega^2 E_a}{\omega_b^2}\frac{1}{d^2+g^2}\coth\frac{\beta\hbar\omega_a}{2}\right] \tag{104}$$

The first term in Eq. (104) represents the contribution of the thermal bath that is directly coupled to resonator b to the decoherence rate. This contribution can be either enhanced ($d > 0$) or suppressed ($d < 0$) due to back-reaction effects. On the other hand, the last term in Eq. (104) [compare with Eq. (71) of Ref. [47]] represents the direct contribution of the driven resonator a. This contribution can be understood in terms of the shift in the effective resonance frequency of resonator a between the two values corresponding to the two coherent states $|\alpha_1\rangle$ and $|\alpha_2\rangle$ (see Ref. [47]).

7. Discussion

We have considered above the case where Ω is small, $K_a = \gamma_{a3} = 0$ and $\gamma_b \ll \omega_b$. In addition, we have assumed that $\gamma_a \ll \gamma_b$ in order to obtain the ISD of X_b, which is given by Eq. (87), and we have assumed the case $\theta = 0$ to obtain the decoherence rate, which is given by Eq. (104). Furthermore, consider for simplicity the case of high temperature where $\beta\hbar\omega_b \ll 1$. For this case Eqs. (87) and (104) can be written in terms of the effective temperatures T_{ISD} and T_{D}

$$\frac{1}{2\pi}\int_{-\infty}^{\infty}\mathrm{d}\omega\, P_{X_b}(\omega) = \frac{2k_{\mathrm{B}}T_{\mathrm{ISD}}}{\hbar\omega_b} \tag{105}$$

$$\frac{1}{\tau_\varphi} = 2\gamma_b|\delta_\alpha|^2\frac{2k_{\mathrm{B}}T_{\mathrm{D}}}{\hbar\omega_b} \tag{106}$$

where

$$\frac{T_{\mathrm{ISD}}}{T} = 1 - \frac{\Omega^2 E_a\Upsilon(d,g)}{\gamma_a\gamma_b}\left(1 - \frac{\omega_b\Xi_a}{\omega_a}\frac{(1+d)^2+g^2}{3d}\right) \tag{107}$$

$$\frac{T_{\mathrm{D}}}{T}=1+\frac{4\Omega^2 E_a}{\omega_b^2}\frac{d}{d^2+g^2}\left(1+\frac{\omega_b\gamma_a\Xi_a}{\omega_a\gamma_b}\frac{1}{d}\right) \tag{108}$$

and

$$\Xi_a=\frac{\beta\hbar\omega_a}{2}\coth\frac{\beta\hbar\omega_a}{2} \tag{109}$$

In terms of $(E_a)_c$, which is given by Eq. (69), one thus has

$$\frac{T_{\mathrm{ISD}}}{T}=1-\frac{E_a}{(E_a)_c}\frac{\omega_b\Upsilon(d,g)}{\sqrt{3}\gamma_b}\left(1-\frac{\omega_b\Xi_a}{\omega_a}\frac{(1+d)^2+g^2}{3d}\right) \tag{110}$$

and

$$\frac{T_{\mathrm{D}}}{T}=1+\frac{4E_a}{\sqrt{3}(E_a)_c}\frac{dg}{d^2+g^2}\left(1+\frac{\omega_b\gamma_a\Xi_a}{\omega_a\gamma_b}\frac{1}{d}\right) \tag{111}$$

These results are valid only to lowest order in Ω, however they may be used in some cases to roughly estimate the lowest possible values of T_{ISD} and T_{D}. As can be seen from Eqs. (110) and (111), the effective temperatures T_{ISD} and T_{D} may take considerably different values. This fact should not be considered as surprising since the system is far from thermal equilibrium and since the underlying mechanisms responsible for ISD reduction and for suppression of decoherence are entirely different. In what follows, we choose the parameters d and g such that the largest reduction in effective temperature is achieved for a given E_a, and use these values to estimate the lowest possible effective temperatures.

7.1. Optimum ISD reduction

For the case of ISD reduction, we consider the case where the term that is proportional to Ξ_a in Eq. (110), namely the term which represents the contribution of the thermal baths that are directly coupled to resonator a, is relatively small, namely the case where $\omega_b\Xi_a\ll\omega_a$. This condition is expected to be fulfilled for the typical experimental situation. Most efficient ISD reduction is achieved by choosing the parameters $g\ll 1$ and $d=1$, for which the term $\Upsilon(d,g)$ obtains its maximum possible value $\Upsilon=1$ (see Fig. 1). For this case Eq. (110) becomes

$$\frac{T_{\mathrm{ISD}}}{T}=1-\frac{\omega_b}{\sqrt{3}\gamma_b}\frac{E_a}{(E_a)_c}\left(1-\frac{4\omega_b\Xi_a}{3\omega_a}\right) \tag{112}$$

By taking

$$E_a=\frac{\sqrt{3}\gamma_b}{\omega_b}(E_a)_c\equiv(E_a)_{\mathrm{ISD}} \tag{113}$$

Eq. (112) yields the lowest possible value of T_{ISD}, which is denoted as $(T_{\mathrm{ISD}})_{\min}$

$$\frac{(T_{\mathrm{ISD}})_{\min}}{T}=\frac{4\omega_b\Xi_a}{3\omega_a} \tag{114}$$

As was mentioned above, the above discussion is based on the approximated result Eq. (110), which expresses T_{ISD} to lowest nonvanishing order in Ω. Such an expansion apparently suggests that the noise contribution due to the thermal bath that is directly coupled to resonator b can be altogether eliminated, leaving thus only the noise contribution of the thermal baths that are directly coupled to resonator a as a lower bound imposed upon T_{ISD} [see Eq. (114)]. Obviously, however, higher orders in Ω have to be taken into account in order to estimate $(T_{\mathrm{ISD}})_{\min}$ more accurately, as was done in Ref. [49], where T_{ISD} was expanded up to fourth order in Ω.

7.2. Decoherence suppression

For the case of decoherence suppression, on the other hand, the term that is proportional to Ξ_a in Eq. (111) is not necessarily small for the common experimental situation. We therefore choose the optimum values of the parameters d and g for the more general case. Using the notation

$$D=\frac{\omega_b\gamma_a\Xi_a}{\omega_a\gamma_b} \tag{115}$$

Eq. (111) reads

$$\frac{T_{\mathrm{D}}}{T}=1+\frac{4E_a}{\sqrt{3}(E_a)_c}f(d,g,D) \tag{116}$$

where

$$f(d,g,D)=\frac{dg}{d^2+g^2}\left(1+\frac{D}{d}\right) \tag{117}$$

In general, the minimum value of the function $f(d,g,D)$ for a given $g>0$ and a given $D>0$ is obtained at

$$d_{\mathrm{m}}=-D-\sqrt{D^2+g^2} \tag{118}$$

and the minimum value is given by

$$f(d_{\mathrm{m}},g,D)=-\frac{1}{2}\tan\left(\frac{\tan^{-1}\frac{g}{D}}{2}\right) \tag{119}$$

The lowest value of $f(d_{\mathrm{m}},g,D)$ is thus obtained in the limit $D\ll g$, for which one finds that $d_{\mathrm{m}}=-g$ and $f(d_{\mathrm{m}},g,D)=-1/2$. Therefore, one concludes that the largest reduction in T_{D} for a given E_a is obtained when

$$\frac{\omega_b^2\Xi_a}{\omega_a\gamma_b}\ll 1 \tag{120}$$

and when $d=-g$. For this case Eq. (111) becomes

$$\frac{T_{\mathrm{D}}}{T}=1-\frac{2}{\sqrt{3}}\frac{E_a}{(E_a)_c} \tag{121}$$

This result indicates that even when all parameters are optimally chosen such that the largest reduction in T_{D} is obtained for a given E_a, no significant reduction in T_{D} is possible unless E_a becomes comparable with $(E_a)_c$. Note, however, that in our analysis of the present case the effect of nonlinear bistability has been disregarded. This approximation can be justified for the case of ISD reduction since, as can be seen from Eq. (113), optimum reduction of the ISD can be achieved well below the bistability threshold provided that $\gamma_b\ll\omega_b$. On the other hand, Eq. (121) indicates that optimum suppression of decoherence can be achieved only very close to the bistability threshold. In this region, however, our approximated treatment breaks down and Eq. (111) becomes inaccurate.

To calculate T_{D} near the bistability threshold we thus numerically evaluate the decoherence rate given by Eq. (99) without assuming that Ω is small or $K_a=\gamma_{a3}=0$. As before, we take $\theta=0$ and consider for simplicity the case where $\beta\hbar\omega_b\ll 1$, for which the effective temperature T_{D} is given by

$$\frac{T_{\mathrm{D}}}{T}=|U_b|^2+\frac{\Gamma_a\omega_b|U_a|^2}{\omega_a\gamma_b}\Xi_a \tag{122}$$

The second term on the right (the term proportional to Ξ_a) represents the contribution of noise originating from the thermal bath that is directly coupled to resonator a. This contribution unavoidably enhances the decoherence rate. On the other hand, the first term $|U_b|^2$, which represents the contribution of noise originating from the thermal bath that is directly coupled to resonator b, can be made either larger or smaller than unity (the value corresponding to the case where the resonators are decoupled from each other, i.e. the case where $\Omega=0$). The added contribution of this noise to the total decoherence rate when Ω is finite comes from back reaction and from frequency mixing due to the nonlinear coupling. When this added contribution constructively interferes with the contribution due to direct coupling between resonator b and the thermal bath the decoherence rate is enhanced. On the other hand, $|U_b|^2<1$ when destructive interference occurs. For that case, suppression of decoherence is possible provided that the contribution of the second term (which is always positive) is kept sufficiently small.

Fig. 2 shows an example calculation of the parameters $|U_b|^2$ and $|U_a|^2$ and the ratio T_{D}/T near bistability threshold of the system. The ratio T_{D}/T is shown for the case where $\beta\hbar\omega_a\ll 1$. The set of system's parameters chosen for this example is listed in the caption of Fig. 2. The stability of the mean filed solution is checked by evaluating the eigenvalues of the matrix W. The dotted sections of the curve T_{D}/T indicate the regions in which the solution is unstable (where at least one of the eigenvalues of W has a negative real part). Near the onset of bistability point [see panel (c4) of Fig. 2] and near jump points in the region of bistability [see panel (d4) of Fig. 2] the ratio T_{D}/T may become relatively small. This behavior can be attributed to critical slowing down, which occurs near these instability points [47]. On the other hand, in the vicinity of these points the solution becomes unstable [see the dotted sections of the curve T_{D}/T in panels (c4) and (d4) of Fig. 2]. When the unstable region is excluded one finds that no significant reduction in the ratio T_{D}/T can be achieved for this particular example (the lowest value is about 0.5).

In the previous example the mean field solutions become unstable close to the onset of bistability. This behavior prevents any significant suppression of decoherence, namely, the ratio T_{D}/T could not be made much smaller than unity. To overcome this limitation the parameter $(E_a)_c$, which is given by Eq. (35), has to be increased without, however, increasing the coupling parameter Ω. We point out below two possibilities to achieve this. In the first one, the parameter K_a is chosen such that $K_a\simeq 2\Omega^2\omega_b/(\omega_b^2+\gamma_b^2)$, and consequently K_a^{eff} becomes very small [see Eq. (27)]. In the second one, which is demonstrated

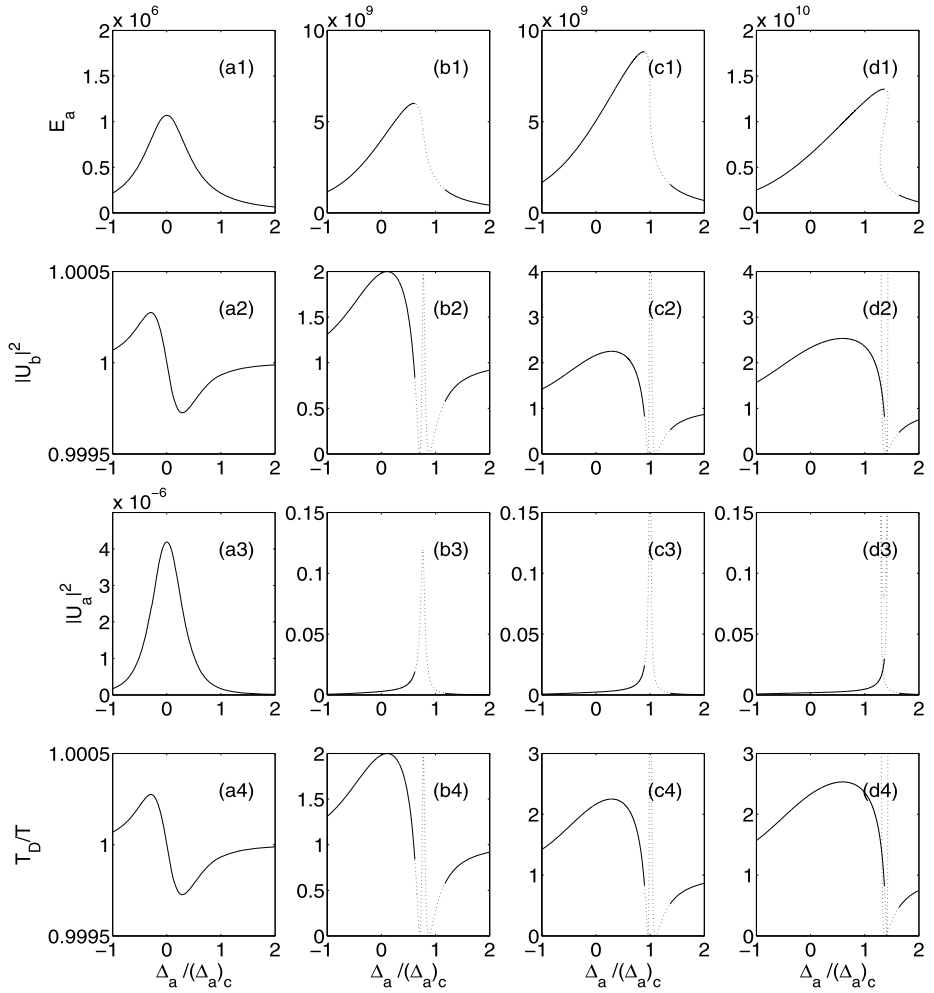

Fig. 2. The factors $|U_b|^2$ and $|U_a|^2$ and the ratio $T_{\rm D}/T$. The driving amplitudes in columns (a), (b), (c) and (d) are $b_p/(b_p)_c = 0.01$, 0.8, 1 and 1.3 respectively. Other system parameters are $\Omega/\omega_a = 10^{-10}$, $\omega_b/\omega_a = 10^{-6}$, $\gamma_b/\omega_b = 10^{-3}$, $K_a = 2\times 2\Omega^2\omega_b/(\omega_b^2+\gamma_b^2)$, $\theta = 0$, $\gamma_{a1}/\omega_b = 10^2$, $\gamma_{a2}/\gamma_{a1} = 10^{-2}$ and $\gamma_{a3} = 0.1\times|K_a^{\rm eff}|/\sqrt{3}$. The ratio $T_{\rm D}/T$, which is plotted in the forth row, is shown for the case $\beta\hbar\omega_a \ll 1$. The dotted sections indicate instability.

in Fig. 3, the nonlinear damping rate γ_{a3} is chosen very close to the largest possible value of $|K_a^{\rm eff}|/\sqrt{3}$ for which bistability is accessible [see inequality (32)]. As can be see from Eq. (35), both possibilities allow significantly increasing the parameter $(E_a)_c$. For the example shown in Fig. 3, the value $\gamma_{a3} = 0.99|K_a^{\rm eff}|/\sqrt{3}$ is chosen and all other parameters are the same as in the previous example (see caption of Fig. 2). As can be seen from panels (c4) and (d4) of Fig. 3, much lower values of the ratio $T_{\rm D}/T$ are achievable in the present example (a lowest value of about 0.02 is obtained at the edge of the region where the solution is stable). This improvement can be attributed to the stabilization effect of the nonlinear damping. As was discussed above, the reduced value of $T_{\rm D}/T$ can be attributed to destructive interference between the direct and indirect noise contributions. Note that for this example the second term on the right hand side of Eq. (122) is about two orders of magnitude smaller than the first term. In other words, the dominant contribution to the total decoherence rate comes from the thermal bath that is directly coupled to resonator b, and consequently the enhancement of decoherence rate due to noise coming from the thermal bath that is directly coupled to resonator a is relatively small.

It is important to point out that implementation of any of the above mentioned methods to suppress decoherence require that the nonlinear parameters of resonator a (K_a and/or γ_{a3}) can be accurately tuned to some specified desired values. Such tuning of nonlinear parameters can possibly become achievable by exploiting effects arising from thermo-optomechanical coupling, as was recently demonstrated in [50]. However, further study is needed in order to investigate possible ways to control decoherence in such systems.

8. Conclusions

In this work we investigate the prospects of employing back-reaction effects for suppression of decoherence in a cavity optomechanical system. We find that no significant suppression of decoherence is achievable when the cavity (resonator a) is

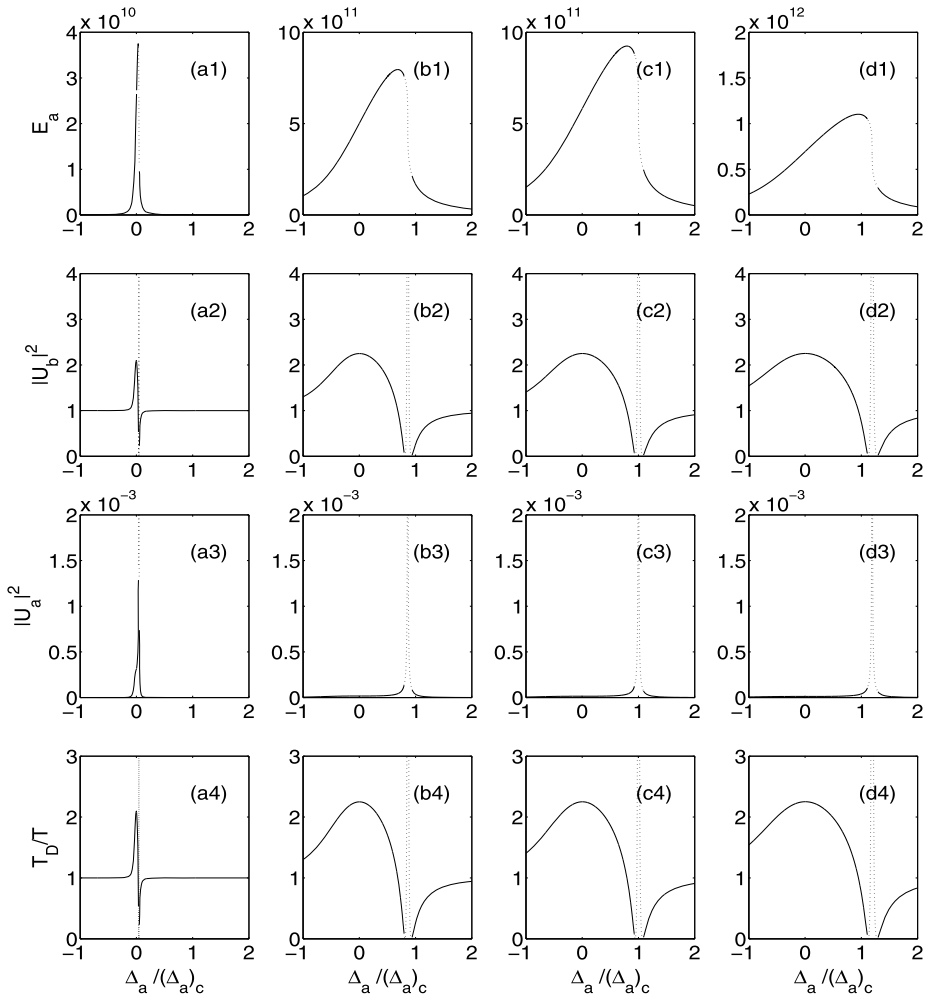

Fig. 3. The factors $|U_b|^2$ and $|U_a|^2$ and the ratio T_{D}/T. In this example $\gamma_{a3} = 0.99 \times |K_a^{\mathrm{eff}}|/\sqrt{3}$ whereas all other parameters are the same as in the previous example [see caption of Fig. 2].

assumed to have a linear response. On the other hand the decoherence rate can be significantly modified when resonator a is driven into nonlinear oscillations. We demonstrate that by very carefully choosing the device's parameters and the driving parameters of resonator a it is possible to suppress decoherence. However, it is important to keep in mind that this happens only in relatively narrow regions in parameters' space, and the case where the decoherence rate is enhanced (rather than being suppressed) is more common.

Acknowledgements

This work is supported by the German–Israel Foundation under grant 1-2038.1114.07, the Israel Science Foundation under grant 1380021 and the European STREP QNEMS Project.

References

[1] Miles Blencowe, Quantum electromechanical systems, Phys. Rep. 395 (2004) 159–222.
[2] Keith C. Schwab, Michael L. Roukes, Putting mechanics into quantum mechanics, Phys. Today (2005) 36–42.
[3] A.D. O'Connell, M. Hofheinz, M. Ansmann, Radoslaw C. Bialczak, M. Lenander, Erik Luceroand M. Neeley, D. Sank, H. Wang, M. Weides, J. Wenner, John M. Martinis, A.N. Cleland, Quantum ground state and single-phonon control of a mechanical resonator, Nature 464 (2010) 697–703.
[4] Roger Penrose, On gravity's role in quantum state reduction, Gen. Relativ. Gravit. 28 (1996) 581–600.
[5] L. Diosi, Models for universal reduction of macroscopic quantum fluctuations, Phys. Rev. A 40 (1989) 1165–1174.
[6] A.J. Leggett, Testing the limits of quantum mechanics: Motivation, state of play, prospects, J. Phys. Condens. Matter 14 (2002) R415.
[7] A.J. Leggett, Anupam Garg, Quantum mechanics versus macroscopic realism: Is the flux there when nobody looks?, Phys. Rev. Lett. 54 (1985) 857–860.
[8] S. Bose, K. Jacobs, P.L. Knight, Preparation of nonclassical states in cavities with a moving mirror, Phys. Rev. A 56 (1997) 4175.
[9] S. Bose, K. Jacobs, P.L. Knight, Scheme to probe the decoherence of a macroscopic object, Phys. Rev. A 59 (1999) 3204–3210.

[10] Dustin Kleckner, Igor Pikovski, Evan Jeffrey, Luuk Ament, Eric Eliel, Jeroen Van Den Brink, Dirk Bouwmeester, Creating and verifying a quantum superposition in a micro-optomechanical system, New J. Phys. 10 (2008) 095020.
[11] Wojciech H. Zurek, Decoherence and the transition from quantum to classical – REVISITED, arXiv:quant-ph/0306072, 2003.
[12] Wojciech Hubert Zurek, Decoherence, einselection, and the quantum origins of the classical, Rev. Mod. Phys. 75 (2003) 715–775.
[13] A.O. Caldeira, A.J. Leggett, Path integral approach to quantum brownian motion, Physica A 121 (1983) 587.
[14] E. Joos, H.D. Zeh, The emergence of classical properties through interaction with the environment, Physik B 59 (1985) 223.
[15] W.G. Unruh, W.H. Zurek, Reduction of a wave packet in quantum brownian motion, Phys. Rev. D 40 (1989) 1071.
[16] W.H. Zurek, Decoherence and the transition from quantum to classical, Phys. Today 44 (1991) 36.
[17] D. Rugar, P. Grutter, Mechanical parametric amplification and thermomechanical noise squeezing, Phys. Rev. Lett. 67 (1991) 699.
[18] R. Almog, S. Zaitsev, O. Shtempluck, E. Buks, Noise squeezing in a nanomechanical duffing resonator, Phys. Rev. Lett. 98 (2007) 78103.
[19] V.B. Braginsky, S.P. Vyatchanin, Low quantum noise tranquilizer for Fabry–Perot interferometer, Phys. Lett. A 293 (2002) 228–234.
[20] Ivar Martin, Alexander Shnirman, Lin Tian, Peter Zoller, Ground-state cooling of mechanical resonators, Phys. Rev. B 69 (2004) 125339.
[21] I. Wilson-Rae, P. Zoller, A. Imamolu, Laser cooling of a nanomechanical resonator mode to its quantum ground state, Phys. Rev. Lett. 92 (2004) 75507.
[22] Aashish A. Clerk, Steven Bennett, Quantum nanoelectromechanics with electrons, quasi-particles and cooper pairs: Effective bath descriptions and strong feedback effects, New J. Phys. 7 (2005) 238.
[23] M.P. Blencowe, J. Imbers, A.D. Armour, Dynamics of a nanomechanical resonator coupled to a superconducting single-electron transistor, New J. Phys. 7 (2005) 236.
[24] D.J. Wineland, J. Britton, R.J. Epstein, D. Leibfried, R.B. Blakestad, K. Brown, J.D. Jost, C. Langer, R. Ozeri, S. Seidelin, J. Wesenberg, Cantilever cooling with radio frequency circuits, arXiv:quant-ph/0606180, 2006.
[25] Florian Marquardt, Joe P. Chen, A.A. Clerk, S.M. Girvin, Quantum theory of cavity-assisted sideband cooling of mechanical motion, Phys. Rev. Lett. 99 (2007) 93902.
[26] H.J. Kimble, Y. Levin, A.B. Matsko, K.S. Thorne, S.P. Vyatchanin, Conversion of conventional gravitational-wave interferometers into quantum nondemolition interferometers by modifying their input and/or output optics, Phys. Rev. D 65 (2001) 022002.
[27] V.B. Braginsky, A.B. Manukin, Ponderomotive effects of electromagnetic radiation, ZhETF 52 (1967) 986–989 (in Russian).
[28] V.B. Braginsky, A.B. Manukin, M.Yu. Tikhonov, Investigation of dissipative ponderomotive effects of electromagnetic radiation, ZhETF 58 (1970) 1550–1555 (in Russian).
[29] Constanze Höhberger Metzger, Khaled Karrai, Cavity cooling of a microlever, Nature 432 (2004) 1002–1005.
[30] S. Gigan, H.R. Böhm, M. Paternostro, F. Blaser, J.B. Hertzberg, K.C. Schwab, D. Bauerle, M. Aspelmeyer, A. Zeilinger, Self cooling of a micromirror by radiation pressure, Nature 444 (2006) 67–70.
[31] O. Arcizet, P.F. Cohadon, T. Briant, M. Pinard, A. Heidmann, Radiation-pressure cooling and optomechanical instability of a micromirror, Nature 444 (2006) 71–74.
[32] D. Kleckner, D. Bouwmeester, Sub-kelvin optical cooling of a micromechanical resonator, Nature 444 (2006) 75–78.
[33] T. Corbitt, D. Ottaway, E. Innerhofer, J. Pelc, N. Mavalvala, Measurement of radiation-pressure-induced optomechanical dynamics in a suspended Fabry–Perot cavity, Phys. Rev. A 74 (2006) 021802.
[34] T. Corbitt, Y. Chen, E. Innerhofer, H. Müller-Ebhardt, D. Ottaway, H. Rehbein, D. Sigg, S. Whitcomb, C. Wipf, N. Mavalvala, An all-optical trap for a gram-scale mirror, Phys. Rev. Lett. 98 (2007) 150802.
[35] A. Schliesser, P. Del'Haye, N. Nooshi, K.J. Vahala, T.J. Kippenberg, Radiation pressure cooling of a micromechanical oscillator using dynamical backaction, Phys. Rev. Lett. 97 (2006) 243905.
[36] J.G.E. Harris, B.M. Zwickl, A.M. Jayich, Stable, mode-matched, medium-finesse optical cavity incorporating a microcantilever mirror: Optical characterization and laser cooling, Rev. Sci. Instrum. 78 (2007) 13107.
[37] A. Naik, O. Buu, M.D. LaHaye, A.D. Armour, A.A. Clerk, M.P. Blencowe, K.C. Schwab, Cooling a nanomechanical resonator with quantum back-action, Nature 443 (2006) 193–196.
[38] A. Schliesser, R. Riviere, G. Anetsberger, O. Arcizet, T.J. Kippenberg, Resolved-sideband cooling of a micromechanical oscillator, Nat. Phys. 4 (2008) 415–419.
[39] C. Genes, D. Vitali, P. Tombesi, S. Gigan, M. Aspelmeyer, Ground-state cooling of a micromechanical oscillator: Comparing cold damping and cavity-assisted cooling schemes, Phys. Rev. A 77 (2008) 033804.
[40] T.J. Kippenberg, K.J. Vahala, Cavity optomechanics: Back-action at the mesoscale, Science 321 (5893) (2008) 1172–1176.
[41] J.D. Teufel, D. Li, M.S. Allman, K. Cicak, A.J. Sirois, J.D. Whittaker, R.W. Simmonds, Circuit cavity electromechanics in the strong coupling regime, Nature 471 (7337) (2011) 204–208.
[42] J.D. Teufel, T. Donner, Dale Li, J.H. Harlow, M.S. Allman, K. Cicak, A.J. Sirois, J.D. Whittaker, K.W. Lehnert, R.W. Simmonds, Sideband cooling micromechanical motion to the quantum ground state, arXiv:1103.2144, 2011.
[43] C.W. Gardiner, M.J. Collett, Input and output in damped quantum systems: Quantum stochastic differential equations and the master equation, Phys. Rev. A 31 (1985) 3761.
[44] Bernard Yurke, Eyal Buks, Performance of cavity-parametric amplifiers, employing Kerr nonlinearities, in the presence of two-photon loss, J. Lightwave Tech. 24 (2006) 5054–5066.
[45] Ady Stern, Yakir Aharonov, Yoseph Imry, Phase uncertainty and loss of interference: A general picture, Phys. Rev. A 41 (7) (1990) 3436–3448.
[46] Y. Levinson, Dephasing in a quantum dot due to coupling with a quantum point contact, Europhys. Lett. 39 (1997) 299–304.
[47] Eyal Buks, Bernard Yurke, Dephasing due to intermode coupling in superconducting stripline resonators, Phys. Rev. A 73 (2006) 23815.
[48] Eyal Buks, M.P. Blencowe, Decoherence and recoherence in a vibrating RF SQUID, Phys. Rev. B 74 (2006) 174504.
[49] M.P. Blencowe, E. Buks, Quantum analysis of a linear DC SQUID mechanical displacement detector, Phys. Rev. B 76 (2007) 14511.
[50] Stav Zaitsev, Ashok K. Pandey, Oleg Shtempluck, Eyal Buks, Forced and self-excited oscillations of optomechanical cavity, Phys. Rev. E 84 (2011) 046605.